ResearchGate

See discussions, stats, and author profiles for this publication at: https://www.researchgate.net/publication/261715085

Time-dependent density functional theory study on the excited-state intramolecular proton transfer in salicylaldehyde

ARTICLE *in* SPECTROCHIMICA ACTA PART A MOLECULAR AND BIOMOLECULAR SPECTROSCOPY · AUGUST 2014

Impact Factor: 2.35 · DOI: 10.1016/j.saa.2014.03.078

CITATIONS
3

READS
25

3 AUTHORS, INCLUDING:

Hang Yin
Jilin University
6 PUBLICATIONS **18** CITATIONS
SEE PROFILE

Ying Shi
Jilin University
33 PUBLICATIONS **244** CITATIONS
SEE PROFILE

All in-text references underlined in blue are linked to publications on ResearchGate, letting you access and read them immediately.

Available from: Hang Yin
Retrieved on: 25 January 2016

Spectrochimica Acta Part A: Molecular and Biomolecular Spectroscopy 129 (2014) 280–284

Contents lists available at ScienceDirect

Spectrochimica Acta Part A: Molecular and Biomolecular Spectroscopy

journal homepage: www.elsevier.com/locate/saa

Time-dependent density functional theory study on the excited-state intramolecular proton transfer in salicylaldehyde

Hang Yin, Ying Shi *, Ye Wang

Institute of Atomic and Molecular Physics, Jilin University, Changchun 130012, China

HIGHLIGHTS

- DFT/TDDFT method has been performed to study the ground and excited states.
- ESIPT was investigated by the characteristic peaks of IR spectra.
- Hydrogen bonded quasi-aromatic chelating ring becoming smaller facilitates ESIPT.
- ESIPT of the SA can be attributed to the electronegativity change of O_1.

GRAPHICAL ABSTRACT

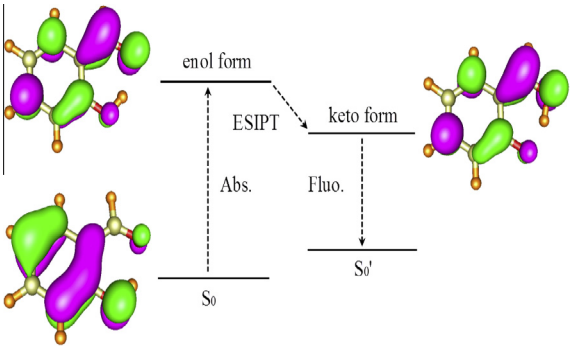

ARTICLE INFO

Article history:
Received 10 February 2014
Received in revised form 8 March 2014
Accepted 21 March 2014
Available online 2 April 2014

Keywords:
Hydrogen bond dynamics
Excited intramolecular proton transfer
DFT/TDDFT

ABSTRACT

Time-dependent density functional theory method was performed to investigate the excited state intramolecular hydrogen bond dynamics of salicylaldehyde (SA). The geometric structures and IR spectra in the ground state S_0 state and the excited state S_1 state of SA are calculated using the density functional theory (DFT) and the time-dependent density functional theory (TDDFT) methods, respectively. In addition, the absorption and fluorescence peaks are also calculated using TDDFT methods. It is noted that the calculated large Stokes shift is in good agreement with the experimental results. Furthermore, our results have demonstrated that the excited state intramolecular proton transfer (ESIPT) process happens upon photoexcitation, which are distinct monitored by the formation and disappearance of the characteristic peaks of IR spectra involved in the formation of hydrogen bonds in different states and in the potential energy curves. We find that the hydrogen bonded quasi-aromatic chelating ring in the excited state becomes smaller which can facilitate the ESIPT process. The results presented here suggest that the ESIPT process of the SA molecule in the excited state can be attributed to the electronegativity change of O_1 induced by excitation.

© 2014 Elsevier B.V. All rights reserved.

Introduction

Intramolecular hydrogen bonding has been a topic of very extensive experimental and computational research for several decades since it plays a crucial role in the photophysics and photochemistry [1–8], which determines the unique structures and functions of biomolecules [9–12]. In the past literatures, it has been demonstrated that excited-state hydrogen bonding can directly influence the microscopic structures and functions of molecules [13–16]. A thorough understanding of intramolecular excited states H-bonding phenomenon may provide a comprehensive explanation of many effects taking place in molecular systems as well. One such important and well-known photochemical

* Corresponding author. Tel.: +86 431 85168817; fax: +86 431 85168816.
E-mail address: shi_ying@jlu.edu.cn (Y. Shi).

http://dx.doi.org/10.1016/j.saa.2014.03.078
1386-1425/© 2014 Elsevier B.V. All rights reserved.

process profoundly influenced by the H-bonding interactions is the excited state intramolecular proton transfer (ESIPT) reaction which was first described by Weller [17]. The authors proposed that along with ESIPT the tautomerization rapidly occurs in the excited-state.

Recently, a number of functional organic molecules based on ESIPT have been investigated extensively [1,18,19]. It is generally believed that the ESIPT process involves that a heterocyclic ring is formed by the intramolecular hydrogen bond between a hydroxyl group and a neighboring proton acceptor. A molecule undergoing ESIPT exhibits characteristic photophysical features such as sub-picosecond time scale and large Stokes shift [17,20,21].

A particular attention is paid to SA molecule that can simultaneously act as the ideal probe to investigate the hydrogen bonding dynamics and may reveal simultaneously the relationship between excited-state hydrogen bonding and proton transfer. SA can also be exploited as a fast and efficient fluorescence probe. Prevenient studies of SA proved that the SA is distinctly different from the methyl salicylate (MS) first proposed by Weller [17]. The three energy levels system of the MS contains the ground state, normal excited state and tautomer excited state. This tautomerism commonly results in an interesting dual fluorescence. However, the SA exhibits single fluorescence and large Stokes shift, which has been proved by experiments [22].

Many research studies have been carried out on this topic. SA has exclusively intramolecular O—H···O hydrogen bonds, which form a rather strong quasi-aromatic chelating ring [23–27]. Previously IR spectra of SA in solid, liquid and gas phases were obtained by Paluszkiewicz et al. [28]. The results confirmed that only intramolecular hydrogen bond can be formed in SA molecules. At the same time, SA was revealed no tendency to self-associate at low temperature. Recently, Boczar et al. performed a theoretical simulation for the ν_s stretching band of SA and its deuterated derivatives, which concerns the adiabatic coupling between the high-frequency O—H (D) stretching and the low-frequency intramolecular O···O stretching modes and the resonance interaction between the O—H and the C—H stretching vibrations in the aldehyde group [29]. Except this, they obtain the IR and Raman spectra which have an agreement with the results of calculations as well. Similarly, Palomar et al. have study a set of o-hydroxybenzoyl compounds (salicylaldehyde, o-hydroxyacetophenone, methylsalicylate and salicylamide) and their parent compounds (phenol, benzaldehyde, acetophenone, methyl benzoate and benzamide) with infrared measurements and quantum chemical calculations, which are analyzed in order to obtain information about the nature of the hydrogen bonding interaction in this family of compounds [25].

It is noteworthy that the results from both experiment and theory in above literatures are about the ground state, focusing on the properties of SA at the ground state. In 2002, Stock and co-workers investigated the ESIPT and internal conversion (IC) of SA molecule experimentally, using the transient absorption measurement and the quantitative fluorescence spectroscopy in aprotic solvent [22]. They suggested that a 45 fs ultrafast process happens in S_1 state, which was assigned to the ESIPT process. What is not clear from the above experiments is why the fluorescence of the SA is the single fluorescence. And the detailed ESIPT process of SA is still worth to be confirmed further.

In the present work, we investigate the ground-state and the excited state structures of SA using the DFT and TDDFT methods, respectively. In addition, the very important information about its absorption spectra and fluorescence spectra have been obtained. The differences of IR spectra between the ground state and the excited state were circumstantiated. Simultaneously, the electronic excitation energy, corresponding to the oscillator strengths in different electronic states, the frontier molecular orbitals and the dominant orbital transition contributions to the electronic states with their percentage were presented.

The potential energy curves along the proton transfer coordinate both in the ground and the excited state were also calculated. Furthermore, our computational results lend strong support to the experimental results of Stock's [22]. We focus attention on studying the proton transfer mechanism of the SA in the excited state in detail.

Computational methods

In the present work, the ground-state and electronic excited-state geometry optimizations were performed by the DFT and TDDFT [30–41] methods respectively. The B3-LYP (Becke's three-parameter hybrid exchange function with Lee–Yang–Parr gradient-corrected correlation) functional and the TZVP basis set (the triple-ζ valence quality with one set of polarization functions) were used in our DFT and TDDFT calculation throughout [42–45]. Fine quadrature grids 4 were employed. Diagonalization of the Hessian determined harmonic vibrational frequencies in the ground state and the excited state. And the excited-state Hession was obtained, with central differences and default displacements of 0.02 Bohr, by numerical differentiation of analytical gradients. In addition, IR intensities were derived from the gradients of the dipole moment. All the electronic structure calculations were carried out using the TURBOMOLE program suite [46].

Results and discussion

Absorption and fluorescence peak

Table 1 shows the calculated absorption peak and emission peak of SA molecule using the TDDFT/B3LYP/TZVP method. It is obvious that the theoretical results are in good agreement with the experimentally measured absorption and emission maxima [22]. The absorption spectrum is calculated by vertical excitation from the ground state to the S_1 state, and the emission spectrum is calculated by emission from the excited state equilibrium geometry to the ground state non-equilibrium geometry.

Moreover, from Table 1, one can clearly see that the Stokes shift by our calculation is 190.77 nm which has a fairly good agreement with the experimental data 188 nm from Stock's work and 184 nm from Nagaoka's work [22,47]. In Stock's work, the author provided evidence of ESIPT in the excited state, which was argued to take place on the 45 fs. Evidence was presented that the delayed rise of the product emission which means the non-radiative transition is the ESIPT.

Optimized geometric structures

To depict the ESIPT of SA, we optimized their geometric conformations at ground state and excited state coming from ESIPT and the results are shown in Fig. 1.

One can clearly see that intramolecular hydrogen bonds of SA can be formed between C_7═O_1 and O_2—H_{pt} in the ground state, whereas they can be formed between C_3═O_2 and O_1—H_{pt} in the

Table 1
Calculated absorption peak and emission peak of SA molecule comparing them with the experimental data [22,47].

	Abs. (nm)	Fluo. (nm)
Exp.[a]	330	518
Exp.[b]	329	513
Theor.	314.79	505.56

[a] means the experimental data from Ref. [22].
[b] means the experimental data from Ref. [47].

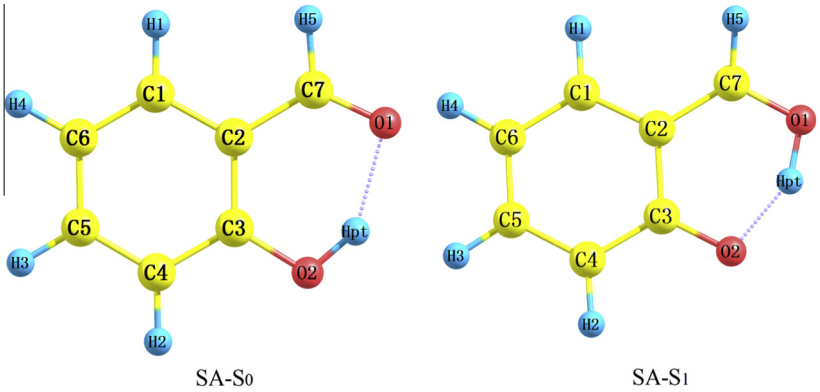

Fig. 1. Schematic plots of the SA structure optimized in the ground and excited state in this work. The numerical values of key geometric parameters are shown in Table 2.

Table 2
Calculated bond lengths (Å) and bond angles (°) of the SA molecule in different electronic state.

	C_2—C_7	C_7—O_1	O_1—H_{pt}	O_2—H_{pt}	O_1—O_2	C_3—O_2	<$C_3C_2C_7$	<$C_2C_3O_2$
S_0	1.45	1.23	1.76	0.99	2.64	1.34	120.32	121.88
S_1	1.44	1.32	1.03	1.56	2.51	1.28	118.26	120.10

excited state. In addition, the numerical values of key geometric parameters of different electronic states can be found in Table 2. Particularly, upon exciting to S_1 excited state the distance between O_1 and H_{pt} decreases from 1.76 Å to 1.03 Å, while that between bond length O_2 and H_{pt} increases from 0.99 Å to 1.56 Å, respectively. The excited state bond angles $C_3C_2C_7$ and $C_2C_3O_2$ are both smaller than the corresponding ground state bond angles. The excited state distance between O_1 and O_2 becomes shorter than the corresponding ground state distance. The changes of bond length and bond angles of the SA indicate that from the ground state to the singlet excited state, the intramolecular C_7═$O_1\cdots H_{pt}$—O_2 breaks, concomitantly accompanying with the formation of an intramolecular C_3═$O_2\cdots H_{pt}$—O_1. The most plausible explanation is that the hydrogen bonded quasi-aromatic chelating ring becomes smaller after exciting. With the decreasing of the distances between atoms, the interactions of involved atoms increase. Therefore, the intramolecular hydrogen bond in the SA molecule facilitates the ESIPT process.

Table 3
The electronic excitation energy (EEE), corresponding oscillator strengths (OS) of the SA molecule in different electronic state and dominant Orbital Transition (OT) contributions to the electronic states with their percentage.

	EEE (nm)	OS	OT
S_1	314.79	0.067	H → L (94.5%)
S_2	313.08	0.000	H-1 → L (97.1%)
S_3	242.34	0.167	H-2 → L (80.9%) H → L + 1 (14.3%)
S_4	212.56	0.193	H → L + 1 (62.1%) H → L + 2 (15.7%) H-2 → L (10.9%) H-2 → L + 1 (5.6%)
S_5	201.29	0.000	H-1 → L + 1 (98.0%)
S_6	196.39	0.180	H-2 → L + 1 (42.5%) H → L + 2 (26.6%) H-3 → L (14.6%) H → L + 1 (13.3%)

Frontier molecular orbitals

To investigate the nature of the excited state, the frontier molecular orbitals are analyzed. From the results listed in Table 3, we know that the S_1 state of the SA corresponds mainly to the HOMO → LUMO transition. In Fig. 2, we show the schematic plots of frontier molecular orbital (HOMO&LUMO) of the SA molecule. It is to be noted that the HOMO and LUMO are respectively the π and π* character. That is to say, the S_1 state is of ππ* feature which is believed to facilitate the proton transfer [2]. It can be seen clearly that the electron density on the carbonyl group in the LUMO in comparison to the HOMO is increased, while that on the hydroxyl group is decreased. Interestingly, as mentioned above, the electronegativity of O_1 atom which is directly involved the ESIPT process increases a lot after exciting to the S_1 state. Furthermore, because of the increasement of O_1 electronegativity after exciting, the electrostatic attraction between O_1 and H_{pt} increases. That is the reason why the ESIPT happens. Therefore, we suggest that the electronegativity change of O_1 due to the intramolecular charge redistribution in the S_1 state is not only tightly associated with changes of the acid-base properties of hydroxyl group and carbonyl group but also induces the ESIPT.

IR spectra

The other aspect relevant to the ESIPT process is the spectroscopic aspect. The vibrational frequencies of the stretching vibrations of C═O and O—H groups that are involved in hydrogen bonds, as is well known, can provide a distinct signature of the hydrogen-bonding dynamics [48]. In the present work, we have calculated the IR spectra (B3LYP/TZVP, scaling factor 0.9630 [49]) of SA molecule which is intramolecular hydrogen bonded in both the ground state and the excited state initially prepared by photoexcitation to S_1 state. The calculated IR spectra in the ground state in the spectral range from 1500 to 3500 cm^{-1}, which contains the

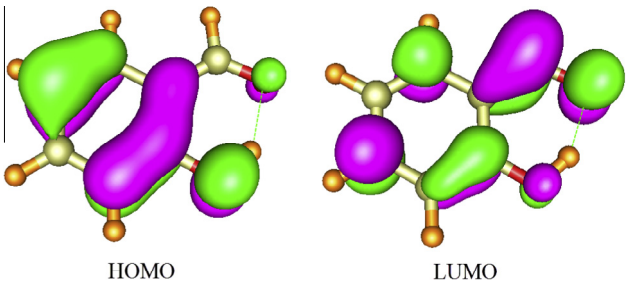

Fig. 2. Schematic plots of molecular orbitals: HOMO and LUMO of SA (B3LYP/TZVP).

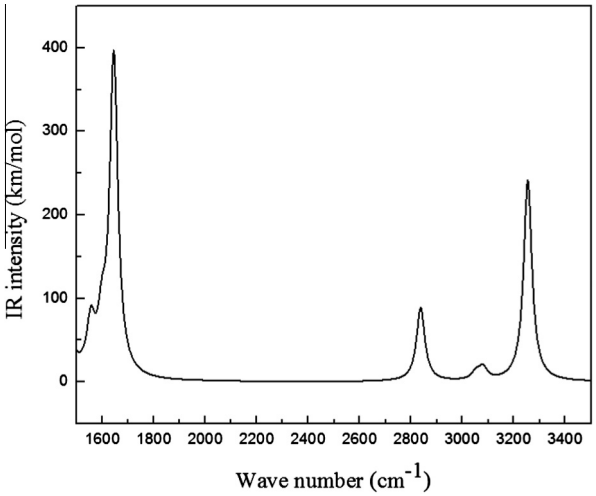

Fig. 3a. Calculated the IR spectra of SA molecules at the ground state.

characteristic peaks of $C_7{=}O_1$ and $O_2{-}H_{pt}$ groups, are shown in Fig. 3a. Respectively, in our calculation, the $C_7{=}O_1$ and $O_2{-}H_{pt}$ stretching vibrational frequency of SA in the ground state is 1643 and 3253 cm^{-1}. The comparison between the present work and Palomar's [25] is shown in Table 4. From Table 4, one can find that the calculation of IR spectra of the present work in the ground state has an agreement with experimental and theoretical data from Palomar's research fairly well. Furthermore, the calculated IR spectra in the excited state at the spectral range from 1500 to 3500 cm^{-1} which differs from that in the ground state markedly is shown in Fig. 3b. It is a remarkable fact that the characteristic peak around 3253 cm^{-1} is disappeared which is assigned as $\nu(O_2{-}H_{pt})$ in the ground state while the new characteristic peak around 2562 cm^{-1} which is assigned as $\nu(O_1{-}H_{pt})$ comes out. Thus, we can conclude that the bond of $O_2{-}H_{pt}$ breaks up and a new bond which should be $O_1{-}H_{pt}$ forms, just as the geometry optimizations shown in Fig. 1. Consequently, as the auxiliary evidences, the IR spectra can correlate well with the result that the H_{pt} transfers from O_2 to O_1.

Potential energy curves

The potential energy curves of the ground state and the excited state for the SA molecule were optimized by fixing the distance between O_2 and H_{pt} (proton transfer coordinate) in different values, which are recorded in Figs. 4a and 4b.

However, there are obvious differences in the potential energy curve between the ground state and electronic states that can legibly describe the experimental observations in terms of the ESIPT process. As shown in Figs. 4a and 4b, the potential energy curves reveal that the stable points in the S_0 state and the S_1 state are corresponding to the coordinate 0.99 Å and 1.56 Å, respectively. It depicts that the structure of SA is not stable after Frank–Condon transition to the S_1 state. To achieve the equilibrium geometry of S_1 state, the H_{pt} transfers from O_2 to O_1, which forms the new hydrogen bond $C_3{=}O_2\cdots H_{pt}{-}O_1$. Therefore, it is distinct that the enol form is stable in S_0 state and the keto form is stable in S_1 state, which is the direct evidence of an ESIPT process happens upon photoexcitation to the S_1 state. Moreover, we also can find that there is only one stable point in the S_1 state. It means that the SA molecule undergoes the ESIPT process directly without normal excited state, which is the reason why the SA exhibits single fluorescence different from the dual-fluorescence MS first proposed by Weller [17]. The potential energy curves can also enlighten on the feasibility of the ground state intramolecular proton transfer of SA. The stable points and corresponding coordinates imply that the intramolecular proton transfer process does not occur in the ground state but the ESIPT is feasible in the S_1 state for the SA molecule.

Table 4
Vibrational frequencies, IR intensities and assignments of SA.

Assignments[a]	ν_{exp}[b]	$\nu_{theor.}$[c]	$\nu_{theor.}$[d]	$A_{theor.}$[e]	$A_{theor.}$[f]
ν(C═O)	1668	1666	1643	331	397
ν(O—H)	3245–3080	3226	3253	225	241

[a] Qualitative normal mode decomposition.
[b] Frequencies (cm^{-1}) from IR spectra of CCl4 and CS2 solutions, from Ref. [25].
[c] Frequencies (cm^{-1}) from B3LYP/6-31G** calculations (scale factor 0.9613) (exp. vs. theor. frequencies: $r = 0.9997$), from Ref. [25].
[d] Frequencies (cm^{-1}) from B3LYP/TZVP calculations of the present work (scale factor 0.9630 [49]).
[e] Theoretical IR intensities (km/mol) at B3LYP/6-31G** level, from Ref. [25].
[f] Theoretical IR intensities (km/mol) at B3LYP/TZVP level, from the present work (scale factor 0.9630 [49]).

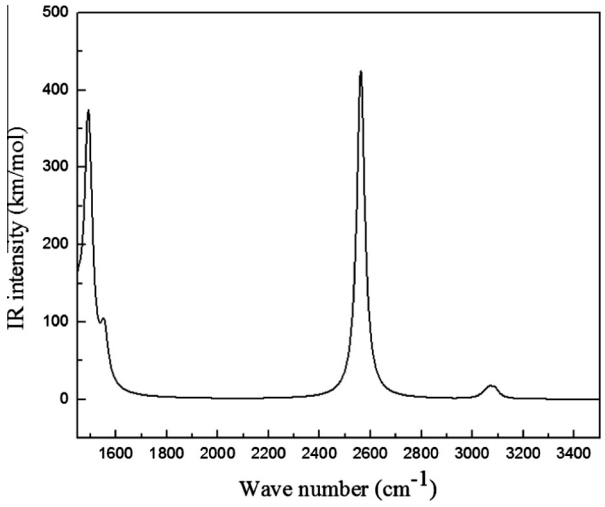

Fig. 3b. Calculated the IR spectra of SA molecule in the excited state.

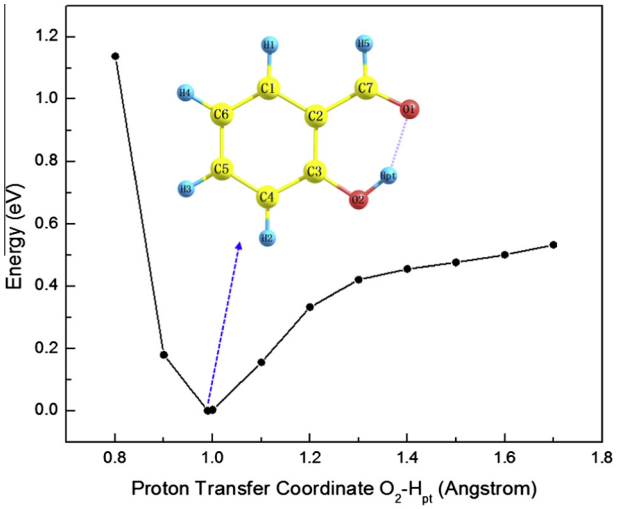

Fig. 4a. Calculated potential energy curves along the proton transfer coordinate in the S_0 state.

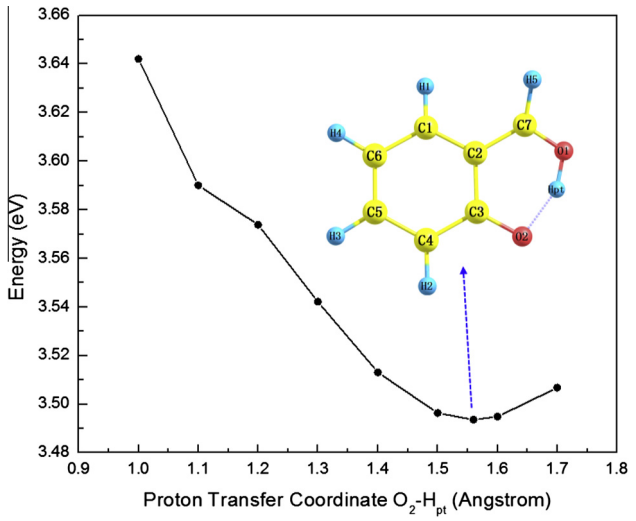

Fig. 4b. Calculated potential energy curves along the proton transfer coordinate in the S_1 state.

Conclusions

The excited state properties of intramolecular hydrogen bonding for SA and its effect on the excited state intramolecular proton transfer were investigated using the TD-DFT method. The geometric structures and energetics of the SA in ground state and the S_1 state were discussed. It is confirmed that the hydrogen bonded quasi-aromatic chelating ring becomes smaller after exciting, which facilitates the ESIPT process.

To investigate the detailed aspects of ESIPT of SA, the vibrational absorption spectra of hydrogen-bonded groups both in ground state and the electronically excited-state are also calculated using the DFT and TDDFT methods. One can note that the SA molecule exhibits the ESIPT process upon photoexcitation to the S_1 state, by comparison IR spectra between ground state and excited state. The formation and disappearance of the characteristic peaks involved in the formation of hydrogen bonds in different states correlate well with the results that the H_{pt} transfers from O_2 to O_1.

All the calculated spectral features are in good agreement with the experimental spectra. The calculated large Stokes shift demonstrates that the SA proton transfer mechanism is reasonable and credible. In addition, the potential energy curves of the ground state and the excited state for the SA molecule were calculated as well. The result is the direct evidence of an ESIPT process happens upon photoexcitation to the S_1 state and explains the single fluorescence spectral features. Furthermore, it also implies that the intramolecular proton transfer process does not occur in the ground state but the ESIPT is feasible in the S_1 state for the SA molecule.

With the aim of investigating the motivation of the ESIPT process of SA, we performed the calculation of frontier molecular orbitals as well. As a consequence, we suggest that the electronegativity change of O_1 due to the intramolecular charge redistribution in the S_1 state induces the ESIPT.

Acknowledgments

This work was supported by the National Basic Research Program of China (973 Program) (2013CB922200) and the National Natural Science Foundation of China (Nos. 11174106 and 10974069) and the Natural Science Foundation of Jilin Province of China (Grant No. 201115018)

This article supported by High Performance Computing Center of Jilin University, China.

References

[1] M.Z. Zhang, D.P. Yang, B.P. Ren, D.D. Wang, J. Fluoresce. 23 (2013) 761.
[2] X. Lan, D.P. Yang, X. Sui, D.D. Wang, Spectrochim. Acta, Part A 102 (2013) 281.
[3] G.L. Cui, Z.G. Lan, W. Thiel, J. Am. Chem. Soc. 134 (2012) 1662.
[4] K.L. Han, G.J. Zhao, Hydrogen Bonding and Transfer in the Excited State, Wiley Online Library, 2011.
[5] M. Huang, Z. Wang, Y. Yang, L. Hao, W. Zhao, X. Gao, L. Fang, W. Zhang, Int. J. Quantum Chem. 107 (2007) 1092.
[6] S.J. Grabowski, Hydrogen Bonding: New Insights, Springer, Dordrecht, The Netherlands, 2006.
[7] M. Sun, J. Chem. Phys. 124 (2006) 054903.
[8] Q. Wang, F. Gao, H.R. Li, S.T. Zhang, Chin. J. Chem. 28 (2010) 901.
[9] S. Goswami, A. Manna, S. Paul, A.K. Das, K. Aich, P.K. Nandi, Chem. Commun. 49 (2013) 2912.
[10] D.P. Yang, L.F. Zhang, J. Phys. Org. Chem. 25 (2012) 1391.
[11] N. Kungwan, F. Plasser, A.J.A. Aquino, M. Barbatti, P. Wolschann, H. Lischka, Phys. Chem. Chem. Phys. 14 (2012) 9016.
[12] J. Catalán, J.C. del Valle, J. Palomar, C. Díaz, J.L. de Paz, J. Phys. Chem. A 103 (1999) 10921.
[13] D. Yang, Y. Liu, D. Shi, J. Sun, Comput. Theor. Chem. 984 (2012) 76.
[14] Y.H. Liu, P. Li, J. Lumin. 131 (2011) 2116.
[15] Y.F. Liu, D.P. Yang, D.H. Shi, J.F. Sun, J. Comput. Chem. 32 (2011) 3475.
[16] Z. Zhou, Y. Qu, A. Fu, B. Du, F. He, H. Gao, Int. J. Quantum Chem. 89 (2002) 550.
[17] A. Weller, Zeitschrift für Elektrochemie, Ber. Bunsen-Ges. Phys. Chem. 60 (1956) 1144.
[18] K.R. Phatangare, V.D. Gupta, A.B. Tathe, V.S. Padalkar, V.S. Patil, P. Ramasami, N. Sekar, Tetrahedron 69 (2013) 1767.
[19] V. Padalkar, P. Ramasami, N. Sekar, Int. Conf. Comput. Sci. 18 (2013) 797.
[20] K. Chevalier, A. Grün, A. Stamm, Y. Schmitt, M. Gerhards, R. Diller, J. Phys. Chem. A 117 (2013) 11233.
[21] S. Mitra, N. Tamai, S. Mukherjee, J. Photochem. Photobiol., A 178 (2006) 76.
[22] K. Stock, T. Bizjak, S. Lochbrunner, Chem. Phys. Lett. 354 (2002) 409.
[23] P. Lipkowski, A. Koll, A. Karpfen, P. Wolschann, Chem. Phys. Lett. 360 (2002) 256.
[24] P. Srivastava, S. Rai, J. Chem. Sci. 111 (1999) 609.
[25] J. Palomar, J. Paz, J. Catalan, Chem. Phys. 246 (1999) 167.
[26] A. Modelli, F. Scagnolari, G. Distefano, Chem. Phys. 250 (1999) 311.
[27] C. Chen, S.F. Shyu, F.S. Hsu, Int. J. Quantum Chem. 74 (1999) 395.
[28] C. Paluszkiewicz, M.J. Wojcik, M. Bala, Bull. Pol. Acad. Sci., Chem. 33 (1985) 361.
[29] M. Boczar, M.J. Wójcik, K. Szczeponek, D. Jamróz, S. Ikeda, Int. J. Quantum Chem. 90 (2002) 689.
[30] M.Z. Zhang, B.P. Ren, Y. Wang, C.X. Zhao, Spectrochim. Acta, Part A 101 (2013) 191.
[31] G.J. Zhao, K.L. Han, Acc. Chem. Res. 45 (2012) 404.
[32] C. Miao, Y. Shi, J. Comput. Chem. 32 (2011) 3058.
[33] G.J. Zhao, K.L. Han, J. Phys. Chem. A 113 (2009) 14329.
[34] Y.F. Liu, J.X. Ding, R.Q. Liu, D.H. Shi, J.F. Sun, J. Comput. Chem. 30 (2009) 2723.
[35] G.J. Zhao, K.L. Han, Biophys. J. 94 (2008) 38.
[36] G.J. Zhao, K.L. Han, J. Comput. Chem. 29 (2008) 2010.
[37] G.J. Zhao, K.L. Han, ChemPhysChem 9 (2008) 1842.
[38] G.J. Zhao, K.L. Han, J. Phys. Chem. A 111 (2007) 2469.
[39] M. Sun, Y. Ding, H. Xu, J. Phys. Chem. B 111 (2007) 13266.
[40] Y. Li, T. Pullerits, M. Zhao, M. Sun, J. Phys. Chem. C 115 (2011) 21865.
[41] P. Song, Y. Li, F. Ma, T.n. Pullerits, M. Sun, J. Phys. Chem. C 117 (2013) 15879.
[42] F. Furche, R. Ahlrichs, J. Chem. Phys. 117 (2002) 7433.
[43] O. Vahtras, J. Almlöf, M.W. Feyereisen, Chem. Phys. Lett. 213 (1993) 514.
[44] B.I. Dunlap, J. Connolly, J. Sabin, J. Chem. Phys. 71 (1979) 3396.
[45] J.L. Whitten, J. Chem. Phys. 58 (1973) 4496.
[46] R. Ahlrichs, M. Bär, M. Häser, H. Horn, C. Kölmel, Chem. Phys. Lett. 162 (1989) 165.
[47] S. Nagaoka, N. Hirota, M. Sumitani, K. Yoshihara, J. Am. Chem. Soc. 105 (1983) 4220.
[48] V. Samant, A.K. Singh, G. Ramakrishna, H.N. Ghosh, T.K. Ghanty, D.K. Palit, J. Phys. Chem. A 109 (2005) 8693.
[49] V. Lukeš, A. Aquino, H. Lischka, J. Phys. Chem. A 109 (2005) 10232.